AIAA JOURNAL
Vol. 38, No. 6, June 2000

Thermo-Mechanical Response of Patched Plates

A. M. Karlsson* and W. J. Bottega†
Rutgers University, Piscataway, New Jersey 08854-8058

A review, unification, and extension of the analysis and results pertaining to patched beam plates subjected to a uniform temperature field (heating and cooling) and in-plane edge force (compressive or tensile), is presented. A self-consistent nonlinear formulation has been derived, which lends itself to an exact analytical solution, to within the context of the model. Three nondimensional parameters are seen to characterize the response of the composite system. These are 1) a loading parameter, 2) a critical temperature, and 3) a critical membrane force. Critical behavior includes bifurcation buckling, asymptotic buckling, and sling-shot buckling, nontrivial ground states, and demarcation and transition in deflection direction. Results for both heating and cooling are consolidated and presented in a unified manner, yielding a broader understanding of the problem of interest.

I. Introduction

NUMEROUS aerospace, mechanical, and electronic structural components consist of a primary base structure with a secondary element bonded to it for the purpose of strengthening, stiffening, or providing thermal or electrical contact. Specific examples are bonded sensors or repair patches on aircraft wings and fuselages or the attachment of electronic components to printed circuit boards. The combination of the primary and secondary structures forms a composite system. Because the structure has been changed with regard to its geometry and structural properties, the structural response can change significantly with the introduction of the patch, with sometimes unanticipated performance as a result. In particular, the local stiffness has been changed, the neutral axis has been moved, and a thermal mismatch between the base structure and the patch may have been introduced. The last two will independently cause local bending, and together can induce novel behavior of the structure.

A number of investigations have been performed concerning various aspects of the integrity of patched structures.[1–13] Among several issues, thermal effects such as thermally induced instability[1,2] and residual stresses[12,13] were investigated. With regard to the former, it was seen[1,2] that bifurcation buckling, asymptotic buckling, or sling-shot buckling can occur. Related work regarding instability of thin, continuously laminated composite structures are treated in Refs. 14–28 and reviewed in Ref. 1.

In the present work a consolidation of selected results pertaining to patched structures subjected to thermomechanical loading is presented. We consider plates that are either in plane-strain or plane-stress configurations (beam plates), which are subjected to a uniform temperature field (corresponding to heating or cooling from a reference temperature) and an in-plane edge load (compressive or tensile). The problems of interest are formulated through a self-consistent nonlinear formulation, which lends itself to an exact analytical solution, within the context of the model. Because of the nonlinearity of the problem, stability must necessarily be assessed. This is done by examination of the second variation of the energy functional along the loading path. Numerical results are presented that elucidate the characteristic behavior of the system and the factors that control such behavior.

Presented as Paper 99-1231 at the AIAA/ASME/ASCE/AHS/ASC 40th Structures, Structural Dynamics, and Materials Conference, St. Louis, MO, 12–15 April 1999; received 10 May 1999; revision received 10 November 1999; accepted for publication 30 November 1999.

*Ph.D. Candidate, Department of Mechanical and Aerospace Engineering; currently Research Associate, Princeton Materials Institute, Princeton University, Princeton, NJ 08540-5211. Member AIAA.

†Associate Professor, Department of Mechanical and Aerospace Engineering. Associate Fellow AIAA.

II. Problem Statement

We begin by summarizing the formulation for the class of problems of interest: the response of patched plates in plane-strain/plane-stress configurations (beam plates) during uniform heating and cooling from some reference temperature. The formulation is adopted from Ref. 1, and hence the specific details can be found therein.

Consider a plate of normalized (half) length $L \equiv 1$ and normalized thickness h, to which a patch of normalized (half) length L_p and normalized thickness h_p is perfectly and centrally adhered, as shown in Fig. 1, where the thicknesses are such that $h + h_p \ll 1$. The composite structure, consisting of the patch plus the base plate, is divided into two regions: the patched region $S_1 : x \in [0, L_p]$ and the unpatched region $S_2 : x \in [L_p, 1]$. The coordinate x is measured from the center of the span and runs along the upper surface of the base plate, as indicated. Thus, the upper surface of the base plate will be used as the reference surface. In what follows, all length scales are normalized with respect to the dimensional (half) length $\bar{L}$ of the undeformed base plate, and the temperature change Θ is normalized with respect to the reference temperature. The base plate and patch are modeled as independent (von Kármán) plates, with the composite structure viewed as an assemblage of the primitive structures. The resulting constitutive relations are presented in Appendix B.

References 1 and 2 show that the (unknown) resultant membrane force at any cross section of the composite structure is uniform throughout the span $[0, L]$. The membrane force is considered positive in tension and is denoted N_0 (In Ref. 1 $N_0 > 0$ corresponds to a compressive membrane force.). Exploiting this result, the formulation for the problems of interest was transformed from a pure displacement formulation, expressed in terms of the in-plane and transverse displacements, to a mixed formulation, expressed in terms of the (uniform) membrane force N_0 and the respective transverse deflections in the patched and unpatched regions $w_1(x)$ and $w_2(x)$ (positive downward). In so doing, the governing differential equations for the transverse deflections take the form

$$w_1^{iv} - k^{*2} w_1'' = 0 \qquad (x \in S_1) \tag{1a}$$

$$w_2^{iv} - k^2 w_2'' = 0 \qquad (x \in S_2) \tag{1b}$$

where

$$k^{*2} = N_0 / D^* \tag{2a}$$

$$k^2 = N_0 / D \tag{2b}$$

D^* and D are given in Appendix B and correspond to the normalized bending stiffnesses of the composite structure in the patched region and the unpatched base plate (measured with respect to their respective centroids), respectively, and superposed primes denote differentiation with respect to x. The associated boundary and matching conditions similarly take the following simplified forms.

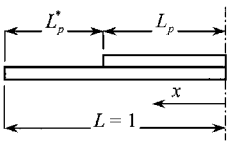

Fig. 1 Geometry of patched plate.

For symmetric deformation:

$$w_1'(0) = 0 \tag{3a}$$

$$\left[D^* w_1''' - N_0 w_1'\right]_{x=0} = 0 \tag{3b}$$

or for antisymmetric deformation:

$$D^* w_1''(0) = 0 \tag{3a′}$$

$$w_1(0) = 0 \tag{3b′}$$

and for both,

$$w_1(L_p) = w_2(L_p) \tag{4a}$$

$$w_1'(L_p) = w_2'(L_p) \tag{4b}$$

$$\left[D^* w_1'' - D w_2''\right]_{x=L_p} = \mathcal{M}_\lambda \tag{4c}$$

$$\left[D^* w_1''' - N_0 w_1'\right]_{x=L_p} = \left[D w_2''' - N_0 w_2'\right]_{x=L_p} \tag{4d}$$

where

$$\mathcal{M}_\lambda \equiv m^* \Theta - \left(\rho^* + \tfrac{1}{2}h\right) N_0 \tag{5}$$

and m^* (the moment per unit temperature exerted on a free structure about an axis through the reference surface) and ρ^* (the location of the centroidal surface with respect to the reference surface) are given in Appendix B.

Upon consideration of Eqs. (1–5), the temperature enters the problem for the transverse deflection through the matching condition for the moments, Eq. (4c). The parameter $\mathcal{M}_\lambda$, as defined by Eq. (5), is thus identified as the loading parameter for the class of problems considered. The loading parameter can be interpreted as a moment applied at the edge of the patch caused by the jump of the neutral surface at this point and caused by the mismatch in coefficients of thermal expansion between the patch and the base structure.

The following integrability condition, which arises from integration of the appropriate strain-displacement relations (Appendix A) and imposition of the corresponding matching conditions for the in-plane displacements, completes the formulation. Hence,

$$u_2(L) - \hat{u}_1(0) = N_0\left(\frac{L_p^*}{C} + \frac{L_p}{C^*}\right) + \left(L_p^*\alpha + L_p\alpha_1\right)\Theta - \left(\rho^* + \frac{h}{2}\right)w'(L_p) - \sum_{i=1}^{2}\int_{S_i}\frac{1}{2}w_i'^2\,\mathrm{d}x \tag{6}$$

together with the associated boundary conditions as follows.

For symmetric deformation:

$$u_1^*(0) = 0 \tag{7a}$$

or for antisymmetric deformation:

$$\hat{u}_1(0) = \hat{\rho} w_1'(0) \tag{7a′}$$

and for both, either

$$u_2(1) = 0 \tag{7b}$$

or

$$N_0 = T_0 \tag{7b′}$$

where T_0 is a prescribed edge load,

$$\hat{u}_1(x) = u_1^*(x) + \rho^* w_1'(x) \tag{8}$$

is the in-plane deflection of the neutral surface of the composite structure within the patched region,

$$\hat{\rho} \equiv m^*\Theta \big| N_0 \tag{9}$$

locates the transverse distance from the centroidal plane to the effective neutral plane of the composite structure (i.e., the plane with vanishing moment), $u_i^*(x)$ is the corresponding in-plane deflection at the reference surface, and $u_i(x)$ is the in-plane deflection of the base plate at its centroid in region S_i. All in-plane deflections are taken positive in the direction of increasing x.

III. Analysis

The solutions for the transverse deflection are linearly proportional to the loading parameter $\mathcal{M}_\lambda$ and take the general form

$$w_i(x) = (\mathcal{M}_\lambda / N_0 \mathcal{H})\Omega_i(x), \qquad (N_0 \neq 0) \quad x \in S_i \quad (i = 1, 2) \tag{10}$$

where the explicit forms of the functions $\Omega_i(x)(i = 1, 2)$ depend on the boundary conditions[1,2] and the expression $\mathcal{H}$ depends on the rotational support conditions as follows:

Hinged edges:

$$\mathcal{H} = \mathcal{H}_{(h)}(N_0; \boldsymbol{S}) = -\sqrt{D^*/D}\cosh\left(k^* L_p\right)\cosh\left(kL_p^*\right) - \sinh\left(k^* L_p\right)\sinh\left(kL_p^*\right) \tag{11a}$$

Clamped edges:

$$\mathcal{H} = \mathcal{H}_{(c)}(N_0; \boldsymbol{S}) = \sinh\left(k^* L_p\right)\cosh\left(kL_p^*\right) + \sqrt{D^*/D}\cosh\left(k^* L_p\right)\sinh\left(kL_p^*\right) \tag{11b}$$

The parameter $\boldsymbol{S}$ appearing in Eqs. (11a) and (11b) represents the set of stiffnesses of the composite structure. (The solution for $N_0 = 0$ may be found in Ref. 1.)

For situations where the edges of the base plate are free to translate in the plane of the plate, the corresponding in-plane edge deflection may be obtained as a function of the applied in-plane edge load and temperature change, by employing Eq. (7b′) and substituting the appropriate form of the solution (10) into Eq. (6). For situations where the edges of the base plate are fixed from translating in the plane of the structure, substitution of the corresponding form of the solution (10) into Eq. (6) gives the nontrivial relationship between the membrane force N_0 and the temperature change Θ. For this case the resulting transcendental expression can be solved numerically for the membrane force for given temperature.

The singularity associated with the vanishing of the function $\mathcal{H}(N_0; \boldsymbol{S})$ appearing in Eq. (10) is associated with bifurcation buckling of the composite structure when the edges of the base plate are free to translate in the plane and with sling-shot buckling when in-plane translation of the edges is prohibited. Thus, the equation

$$\mathcal{H}(N_0, \boldsymbol{S}) = 0 \tag{12}$$

can be interpreted as the associated characteristic equation, with roots $N_0 = N_{\mathrm{cr}}(<0)$. Equations (11a) and (11b) show that N_{cr} is independent of the temperature and the coefficients of thermal expansion.

As the transverse deflection (10) is linearly proportional to the loading parameter $\mathcal{M}_\lambda$, it is evident that vanishing of the loading parameter, $\mathcal{M}_\lambda = 0$, is associated with uniform vanishing of the transverse deflection of the structure. Hence, vanishing of the loading parameter is associated with flat configurations of the deforming structure. When $\mathcal{M}_\lambda$ vanishes, we can, for the particular case where $N_0 = N_{\mathrm{cr}}$, define the corresponding critical temperature $\Theta = \Theta_{\mathrm{cr}}$ from Eq. (5). Hence,

$$\Theta_{\mathrm{cr}} \equiv \left(\rho^* + \tfrac{1}{2}h\right)N_{\mathrm{cr}} \big| m^* \tag{13}$$

The critical temperature is closely associated with the characterization of the structural response of the composite system and will be discussed in Secs. IV and V.

Equation (5) shows that $\mathcal{M}_\lambda$ vanishes for an appropriate ratio of N_0 and Θ provided that the sign of the thermal and mechanical components of the loading parameter are the same for a given configuration. Therefore, for situations where the edges of the base plate are such that in-plane translation is allowed, a loading program can be constructed in such a way that the plate remains flat throughout the loading sequence. For situations where the edges of the base

plate are prohibited from in-plane translation, the membrane force and temperature cannot be prescribed independently, but are related through the integrability condition (6).

When the loading parameter $\mathcal{M}_\lambda$ and the characteristic function $\mathcal{H}$ vanish simultaneously, the solution for the transverse deflection takes the form

$$w_i(x) = A_0\hat{\Omega}_i(x), \qquad x \in S_i \quad (i = 1, 2) \tag{14}$$

where the amplitude A_0 is a constant and the explicit forms of the functions $\hat{\Omega}_i(x)(i = 1, 2)$ depend on the boundary conditions.[1,2] When the edges are free to translate in the plane, the amplitude A_0 is indeterminate when $\mathcal{M}_\lambda = \mathcal{H} = 0$ and corresponds to bifurcation buckling. When the edges of the base plate are fixed with regard to in-plane translation, the amplitude A_0 can take on two values, and the situation where $\mathcal{M}_\lambda = \mathcal{H} = 0\,(\Theta > 0)$ corresponds to sling-shot buckling. Such phenomena will be discussed further in Sec. IV. For negative temperature changes ($\Theta < 0$) the characteristic function $\mathcal{H}$ will not vanish for fixed supports (clamped or pinned) because Eq. (12) is satisfied only when $N_0 < 0$.

As multiple equilibrium configurations for a given value of the load are possible, it is necessary to establish the stability or instability of these configurations. In this regard, stability is assessed by examination of the second variation of the potential energy of the system. A particular configuration will be considered stable if the second variation of the total energy is positive definite for that state, in the context of perturbations away from it. Toward this end, a stability criterion was established in Ref. 1 and involved perturbations in terms of a small moment about an axis through the reference surface at the edge of the patch. For the class of problems of interest, the stability criterion reduces to the following:

An equilibrium configuration is stable if $\mathcal{F}/N_0 > 0$

and is unstable otherwise (15)

where

$$\mathcal{F} = \tfrac{1}{4}\left(f_{\mathcal{A}}^2 k^* \sinh 2k^* L_p + f_{\mathcal{B}}^2 k \sinh 2kL_p^*\right) \tag{16}$$

$$f_{\mathcal{A}} = \mathcal{A}/\mathcal{H} \tag{17a}$$

$$f_{\mathcal{B}} = \mathcal{B}/\mathcal{H} \tag{17b}$$

$$\mathcal{B} = \sinh(k^* L_p) \tag{18a}$$

Hinged supports:

$$\mathcal{A} = \mathcal{A}_h = \sqrt{D^*/D}\cosh(kL_p^*) \tag{18b}$$

Clamped supports:

$$\mathcal{A} = \mathcal{A}_c = -\sqrt{D^*/D}\sinh(kL_p^*) \tag{18b'}$$

and $\mathcal{H} = \mathcal{H}_h$ or $\mathcal{H}_c$ is the characteristic function for the support condition indicated.

IV. Response of Representative Structures

We next present a consolidation of characteristic results for the class of problems of interest, based on analytical solutions described in the preceding section. Results pertaining to both heating above and cooling below the reference temperature are presented in a unified manner, giving an overall picture of the response of these structures under thermomechanical loading conditions. As the general characteristics of the response are found to be common for both rotational support conditions considered (i.e., for both clamped and hinged rotational edge conditions), the representative results presented herein are limited to clamped conditions at the edge of the base plate, for brevity. However, both free and fixed in-plane support conditions are considered. We thus present results corresponding to both clamped-free and clamped-fixed support conditions at the edge of the base plate. For brevity, the discussion is limited to representative structures with normalized thicknesses $h_p = h = 0.05$, modulus ratio (patch to base plate) $E_0 = 1$, and relative patch length $L_p = 0.8$. To isolate the influence of the ratio of thermal expansion coefficients (patch to base plate) α_0 on the response of the structure, results corresponding to $\alpha_0 = \frac{1}{2}$, 1, and 2 are presented and discussed. Examination of the behavior of the critical parameters N_{cr} and Θ_{cr}, as functions of various structural parameters, allows for an extension of the results of the present section and a characterization of the behavior of a broad range of structures. This is done in Sec. V.

A. Edges Free to Translate in Plane

We first consider the situation where the edges of the base plate are free to allow in-plane edge deflections. For this case we examine the response of the structure under two types of loading scenarios: 1) the plate is loaded on its edges by a controlled in-plane force while it is maintained at a fixed temperature, and 2) the in-plane edge force and the applied temperature field are both controlled such that the loading parameter maintains a constant value.

1. *Edge-Force Controlled Loading in a Fixed Temperature Field*

Consider first the case of a patched plate subjected to a controlled in-plane edge force in a fixed temperature field. For this case, the normalized edge force N_0 is displayed as a function of the associated in-plane edge deflection $u_L \equiv u_2(0)$ for a range of (positive and negative) temperatures for $\alpha_0 = \frac{1}{2}$, 1, and 2 in Figs. 2a, 2b, and 2c, respectively. In each case, one can see that the slopes of the loading paths asymptotically approach a common limiting value for $N_0 > 0$, which is independent of both Θ and α_0. These slopes correspond to the limiting global axial stiffness of the composite structure. For the case of compressive loading ($N_0 < 0$) from the unloaded state, all paths are seen to asymptotically approach the line $N_0 = N_{cr} = -36.3$ regardless of the values of Θ and α_0. This corresponds to asymptotic buckling as $N_0 \to N_{cr}$. As will be seen, the line $N_0 = N_{cr}$ corresponds to the secondary path, following bifurcation, of the path corresponding to the critical temperature for that structure and hence corresponds to bifurcation buckling, with the deflection evidently increasing without bound, within the context of the model. The primary path for this case (not shown) is a straight line corresponding to the limiting axial stiffness. [A second critical load is found at $N_{cr} = -194.6$. However, Refs. 1 and 2 show that for edge-force controlled loading compressive membrane forces with magnitudes exceeding the lowest critical force cannot be reached in the case of kinematically free boundaries (unless the system is artificially constrained until the first N_{cr} is surpassed).]

The loading paths, expressed in terms of the in-plane edge force N_0 as a function of the transverse centerspan deflection $w_0 \equiv w_1(0)$, are displayed in Figs. 3a and 3b for $\alpha_0 = \frac{1}{2}$ and 2, respectively. (For the case of $\alpha_0 = 1$, the centerspan deflection is independent of the temperature, yielding positive deflection for tensile forces and negative deflection for compressive forces.[1,2]) The figures show that at the critical temperature ($\Theta_{cr} = 7.57$ for $\alpha_0 = \frac{1}{2}$ and $\Theta_{cr} = -3.78$ for $\alpha_0 = 2$) the transverse centerspan deflection is independent of the membrane force (within the resolution of the figures) for $N_0 > 0$ and also for $N_0 < 0$ until the critical membrane force is reached ($N_{cr} = -36.3$). At the critical load a bifurcation of the path occurs, with w_0 increasing without bound through either positive or negative values. For temperatures other than the critical temperature, the load paths are seen to asymptotically approach the path for Θ_{cr}, culminating in asymptotic buckling as the critical load is approached.

The critical temperature divides the sense of the structural response between upward and downward deflection changes. Thus, when the patched plate is subjected to its critical temperature, the thermal load causes the composite structure to behave as an effectively perfect structure (i.e., as an initially flat, unpatched beam plate subjected to an in-plane compressive force). When the structure is subjected to temperatures other than the critical temperature, the patched plate behaves in a manner similar to a uniform structure with imperfections. Furthermore, the sign of the deflection change is associated with the sign of the loading parameter $\mathcal{M}_\lambda$, where the sign of $\mathcal{M}_\lambda$ is the result of the competition between its thermal component and its mechanical component, which may be seen in Eq. (5).[1,2]

2. *Edge-Force Controlled Loading with Fixed Loading Parameters*

Consider now the situation where the temperature Θ and membrane force N_0 are controlled in such a manner that the loading parameter $\mathcal{M}_\lambda$ remains constant. Such a balance may be achieved

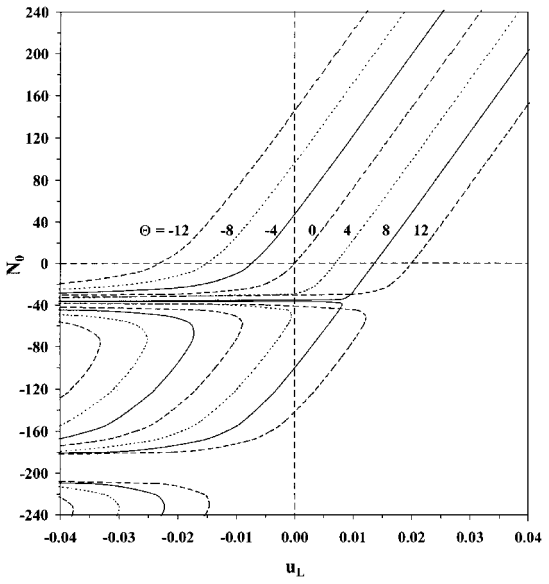

a) $\alpha_0 = \frac{1}{2}$

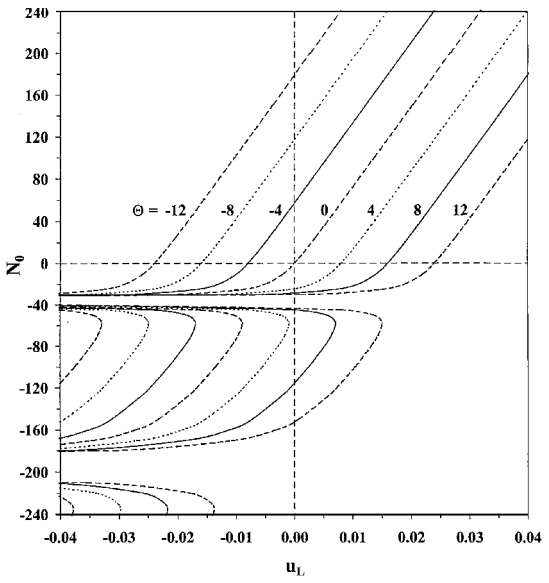

b) $\alpha_0 = 1$

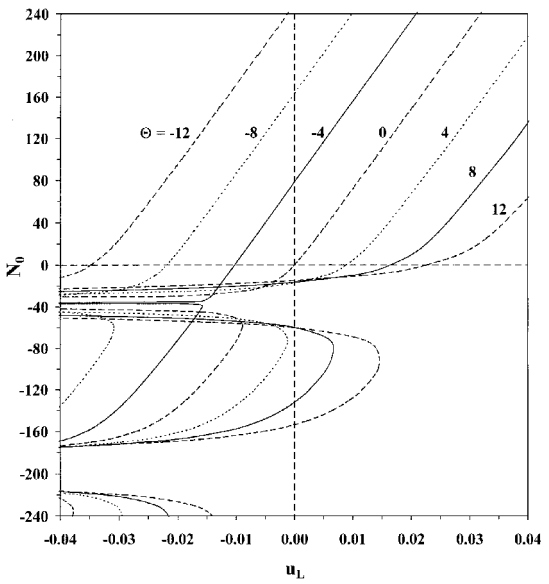

c) $\alpha_0 = 2$

Fig. 2 Normalized membrane force N_0 vs normalized in-plane edge displacement u_L for various normalized temperatures Θ ($L_p = 0.8$).

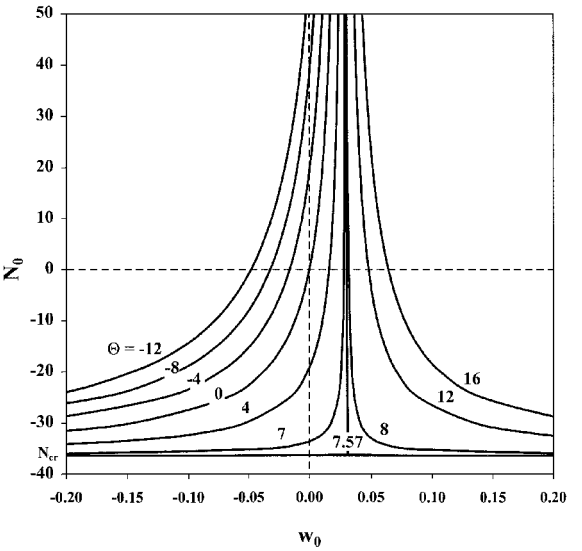

a) $\alpha_0 = \frac{1}{2}$

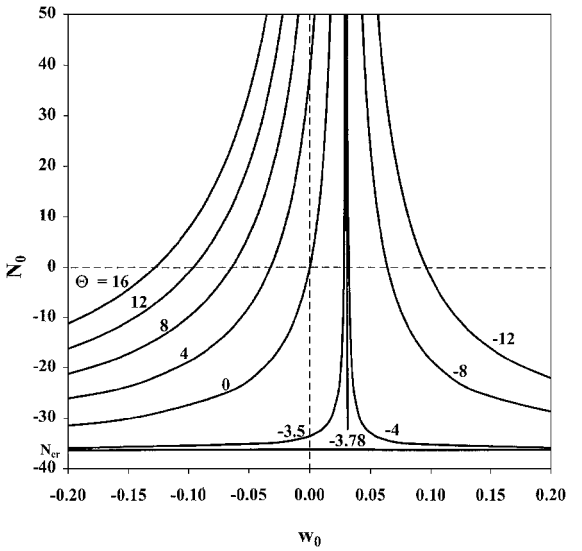

b) $\alpha_0 = 2$

Fig. 3 Normalized membrane force N_0 vs normalized transverse centerspan displacement w_0 for various values of the normalized temperature Θ (clamped-free supports, $L_p = 0.8$).

through Eq. (5), for example, if N_0 is changed monotonically and the value of $m^*\Theta$ is adjusted accordingly. [It follows from equations (B7) and (B5) that, for the current structural parameters, if $\alpha_0 = 1$ then $m^* = 0$, if $\alpha_0 < 1$ then $m^* < 0$, and if $\alpha_0 > 1$ then $m^* > 0$.] This situation is illustrated in Fig. 4, where the membrane force N_0 is displayed as a function of the centerspan deflection w_0 for various values of the load parameter $\mathcal{M}_\lambda$.

Figure 4 shows that vanishing loading parameter $\mathcal{M}_\lambda = 0$ corresponds to vanishing of the transverse deflection for all membrane forces considered, as was anticipated in Sec. III. As for the case of edge-force controlled loading in a fixed temperature field, the intersection of the corresponding primary path with the line $N_0 = N_{cr}$ corresponds to a bifurcation point. Thus, for $\mathcal{M}_\lambda = 0$ the structure remains flat until $N_0 = N_{cr}$ at which point bifurcation buckling occurs. For nonvanishing loading parameters, $\mathcal{M}_\lambda < 0$ corresponds to downward deflections of the structure, while $\mathcal{M}_\lambda > 0$ corresponds to upward deflections. The magnitude of the centerspan deflection is symmetric with respect to the loading parameter. Furthermore, if a structure is loaded with a compressive edge force, such that $\mathcal{M}_\lambda \neq 0$, it will buckle asymptotically, and N_{cr} is never exceeded. Finally, for positive membrane force the deflection approaches that of the deflection for a structure loaded with vanishing loading parameter. [Comparing the present results to the classical results for (unpatched) beam plates, the magnitude of $\mathcal{M}_\lambda$ describes

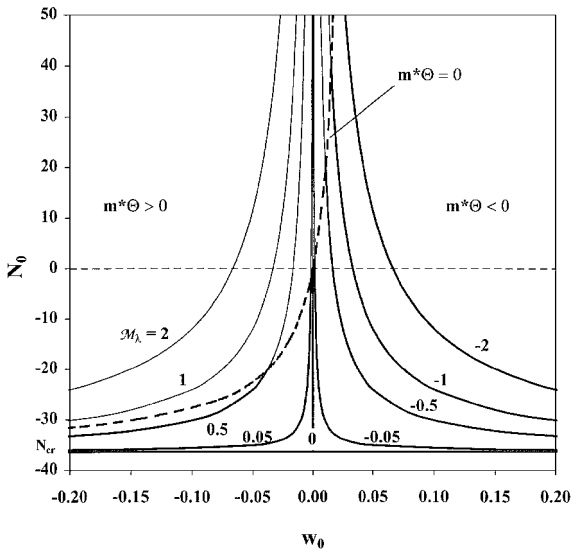

Fig. 4 Normalized membrane force N_0 vs normalized transverse centerspan displacement w_0 for various values of the loading parameter $\mathcal{M}_\lambda$ (clamped-free supports, $L_p = 0.8$).

how far the structure is from being perfect, with $\mathcal{M}_\lambda = 0$ corresponding to a perfect structure.]

B. Edges Fixed from In-Plane Translation

We recall from prior discussion that, when the supports prohibit translation of the edges of the base plate, only discrete combinations of membrane forces and temperatures correspond to equilibrium configurations of the composite structure. Specifically, the membrane force N_0 is solved numerically, as roots of the integrability condition, Eq. (6), with $u_L = 0$ for each given temperature Θ. Thus, for a given temperature the corresponding membrane forces are found where the appropriate isotherm intersects $u_L = 0$ in Figs. 2a–2c. Figures 2a–2c show that, for the range of temperatures considered, either one or three equilibrium configurations are possible for a given temperature.

The three possible equilibrium paths are shown in Figs. 5a–5c, where the temperature is displayed as a function of the centerspan deflection w_0 for $\alpha_0 = \frac{1}{2}$, 1, and 2, respectively. In each case the branches are numbered 1, 2, and 3, as indicated. Branch 1 is associated with the equilibrium path achieved upon loading from the reference state through either positive or negative temperatures. Branches 2 and 3 are maintained for higher (positive) temperatures, where branch 3 corresponds to the one with highest membrane force. Branches 2 and 3 are connected, but are treated as separate branches for clarity. Upon comparison of the corresponding branches discussed in Refs. 1 and 2 with those of Figs. 5a–5c of the present discussion, it is evident that the equilibrium paths associated with cooling are actually part of the first of the multiple branches associated with heating.

Because multiple equilibrium configurations are possible, we must assess the stability of the equilibrium configurations corresponding to each branch. In this regard, the stability of each branch was established using the criterion of Ref. 1 summarized at the end of Sec. III. Correspondingly, in Figs. 5a–5c the stable parts of the branches are indicated as solid lines, and the unstable parts are indicated as dashed lines.

Consider the case of a heated structure with modulus ratio $\alpha_0 = \frac{1}{2}$, as shown in Fig. 5a. Starting from the reference temperature and subsequently increasing the temperature, the centerspan deflection is seen to follow that of the first branch and is always negative (upward). Once the critical temperature is reached, branch 1 becomes unstable while branch 2 becomes stable. Hence, when the surrounding temperature becomes equal to the critical temperature, the plate slingshots from upward deflections (negative) to downward deflections (positive). Sling-shot buckling occurs when the applied temperature equals that of the critical temperature $\Theta = \Theta_{cr}$, regardless of whether the critical temperature is reached through

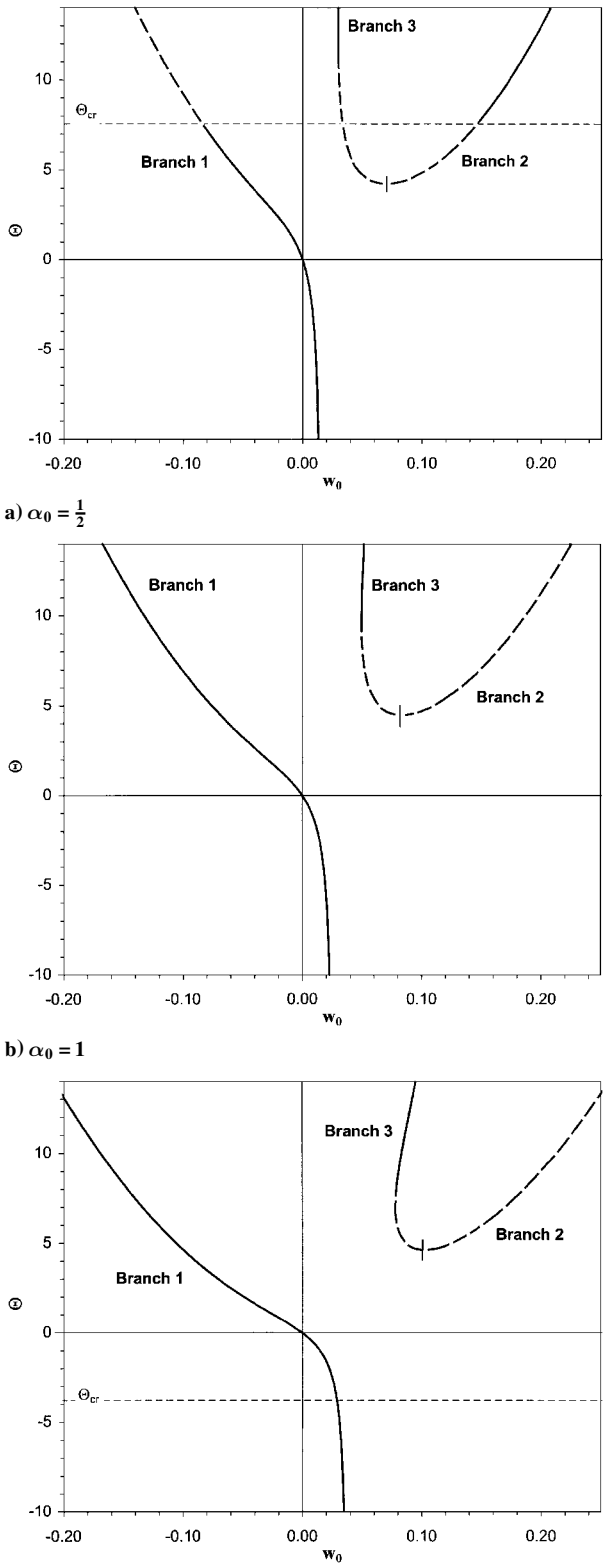

Fig. 5 Normalized temperature Θ vs the normalized transverse displacement w_0 for the first three branches of the equilibrium paths ($L_p = 0.8$) (clamped-fixed supports; – – –, corresponding to unstable configurations).

increasing or decreasing the surrounding temperature. As was discussed in Ref. 1, at sling-shot buckling the membrane force equals the critical membrane force and never surpasses it. A positive critical temperature can only exist for the case of $\alpha_0 < 1$, which follows from Eq. (13). For a structure that does not possess a positive critical temperature, such as $\alpha_0 = 1$ and 2, the centerspan deflection will be negative (upward) for all positive temperatures, and sling-shot buckling does not occur, as seen in Figs. 5b and 5c. (For all cases

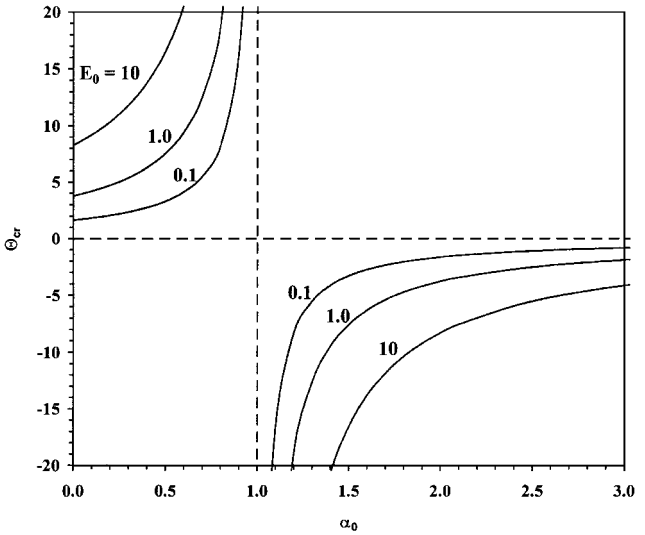

a) Various relative stiffnesses ($L_p = 0.8, h = 0.05$)

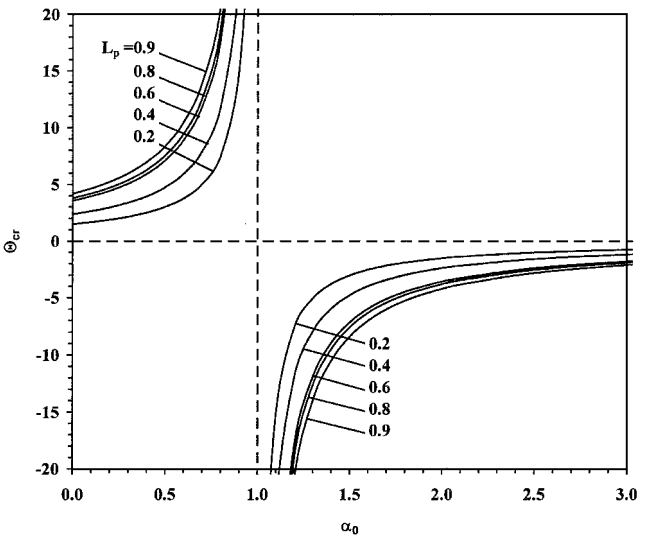

b) Various patch lengths ($E_0 = 1, h = 0.05$)

Fig. 6 Critical temperature Θ_{cr} corresponding to the first critical membrane force for symmetric deformation vs the ratio of coefficients of thermal expansion α_0 (clamped supports).

a part of the third branch is seen to be stable, but this configuration was seen not to be practically achieved.[1])

For the case of cooling, Figs. 5 show that the transverse centerspan deflection is positive for all cases considered, regardless of the value of α_0, and that the existence of a negative critical temperature does not affect the response of the system (A broad range of structures subjected to cooling was examined in Ref. 2, but the results are not repeated here for brevity.)

V. Behavior of the Critical Parameters

Section IV showed that the values of the critical membrane force N_{cr} and critical temperature Θ_{cr} characterize the response of the systems of interest. The parameters are functions of the structural properties of the patched plate, where the properties include the relative length of the patch and the stiffnesses of the composite structure. In this section we will investigate how the critical parameters are affected by the structural properties. By doing so, we extend the results for the representative structure, presented in Sec. IV, to a range of structures. To this end, we will in each case set the thicknesses as $h_p = h = 0.05$. To vary the relative stiffness of the patch, several orders of magnitude of the modulus ratio E_0 are considered. In this way the behavior of a broad range of structures is captured. For brevity, we will only discuss the case of edges being clamped with the regard to rotations.

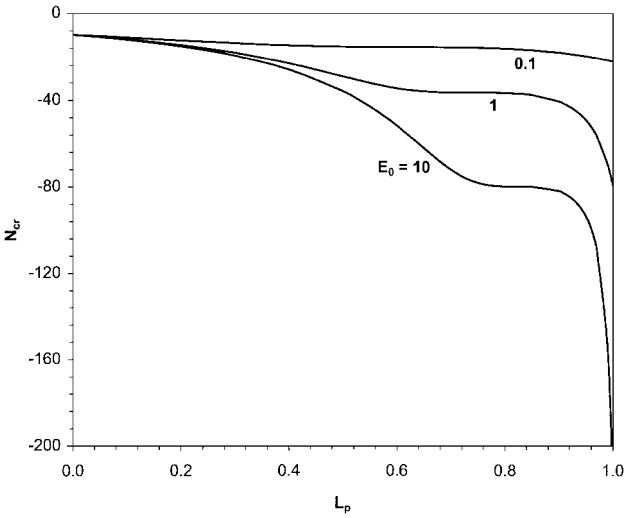

Fig. 7 First critical membrane force N_{cr} for symmetric deformation vs patch length L_p for $E_0 = 0.1, 1, 10$ (clamped supports).

The critical temperature Θ_{cr} corresponding to the lowest critical membrane force for symmetric deformation is displayed as a function of α_0 in Figs. 6a and 6b. Results are shown for various values of the modulus ratio E_0 in Fig. 6a and for a range of patch lengths in Fig. 6b. It may be seen for both cases that the paths are asymptotic to the line $\alpha_0 = 1$ ($m^* = 0$), with no finite value of the critical temperature at $\alpha_0 = 1$. Thus, no critical temperature exists at $\alpha_0 = 1$. The range $\alpha_0 < 1$ ($m^* < 0$) yields positive critical temperatures, whereas $\alpha_0 > 1$ ($m^* > 0$) yields negative critical temperatures.

Finally, the lowest critical membrane force N_{cr} is displayed as a function of the relative patch length L_p in Fig. 7 for the modulus ratios $E_0 = 0.1, 1, 10$. The figure shows that the magnitude of the critical membrane force increases with increasing patch length, particularly for the case of a relatively stiff patch as $L_p \rightarrow 1$.

VI. Conclusion

A review, unification and extension of the analysis and response of patched beam plates subjected to a uniform temperature field (heating and cooling) in combination with a membrane load (tensile or compressive), has been presented. The response of the composite system is described through a self-consistent formulation, including a mathematical model of the system in terms of an assemblage of the base structure and the patch. The resulting nonlinear problem is solved analytically. Thus, the results are exact within the context of the model. Results pertaining to both heating above and cooling below the reference temperature were presented in a unified manner, giving an overall picture of the response of these structures under thermomechanical loading conditions.

The response of the structure may be characterized through three nondimensional parameters: 1) a loading parameter, 2) a critical temperature, and 3) a critical membrane force. All transverse deflections were shown to be proportional to the loading parameter, thus a vanishing loading parameter corresponds to uniformly vanishing transverse deflections. As a consequence of this, it is possible to construct a loading sequence such that the transverse deflection vanishes throughout the loading program, for situations where the edges of the base plate are free to translate in the plane of the structure. A critical temperature can exist for both heating and cooling, depending on the structural parameters of the system, and it is associated with the transition in the direction of the transverse deflection. The critical temperature, together with the (compressive) critical membrane force, is associated with various types of buckling of the structure. These include bifurcation buckling, asymptotic buckling, and sling-shot buckling.

The response of the composite structure was shown to be highly dependent on the type of translational support condition (whether free or fixed with regard to motions in the plane of the structure). When the edges of the base plate are free to translate in the plane, it was seen that, at the critical temperature, the centerspan deflection is

effectively independent of the membrane force for tension and also for compression until the critical level of the membrane force is achieved. Thus, when a structure is subjected to the critical temperature, it behaves as an effectively perfect structure (in the sense of a flat, unpatched beam plate). For temperatures other than the critical temperature, the load paths were seen to asymptotically approach the path corresponding to the critical temperature, culminating in asymptotic buckling as the critical load is approached. The global axial stiffness of the structure, at the critical temperature, was seen to be the limiting global axial stiffness at any other temperature, with the limiting stiffness approached asymptotically for temperatures other than the critical temperature. When the edges of the structure are prohibited from moving in the plane, the phenomenon of sling-shot buckling, associated with the system jumping from one equilibrium path to another, occurs when the surrounding temperature reaches a positive critical temperature. This type of behavior, however, was seen not to occur during cooling. The sole equilibrium path associated with cooling of a given structure is, in fact, an extension of the first of the multiple branches associated with heating.

Appendix A: Deformation—Displacement Relations

Strain-displacement and curvature-displacement relations of the centerline of the base plate and the patch are, respectively

$$e_i = u_i' + \tfrac{1}{2}w_i'^2, \qquad x \in S_i \quad (i = 1, 2) \tag{A1a}$$

$$\kappa_i = w_i'', \qquad x \in S_i \quad (i = 1, 2) \tag{A1b}$$

$$e_p = u_p' + \tfrac{1}{2}w_p'^2, \qquad x \in S_1 \tag{A1c}$$

$$\kappa_p = w_p'', \qquad x \in S_1 \tag{A1d}$$

where $h \ll 1$ and $h_p \ll 1$ correspond to the normalized thickness of the base panel and patch, respectively.

In-plane displacements and membrane strains at the reference surface are

$$u_i^*(x) = u_i(x) + \tfrac{1}{2}hw_i' \qquad (i = 1, 2) \tag{A2a}$$

$$u_p^*(s) = u_p(x) - \tfrac{1}{2}h_p w_p' \tag{A2b}$$

$$e_i^*(x) = e_i(x) + \tfrac{1}{2}h\kappa_i \qquad (i = 1, 2) \tag{A2c}$$

$$e_p^*(x) = e_p(x) - \tfrac{1}{2}h_p\kappa_p \tag{A2d}$$

(Superposed primes indicate total differentiation with respect to x.)

Appendix B: Constitutive Relations and Stiffnesses

Normalized membrane force $N_1^*(x)$ and normalized bending moment $M_1^*(x)$ in the patched portion of the composite structure are as follows:

$$\begin{aligned} N_1^*(x) &= C^* e_1^*(x) + B^*\kappa_1^*(x) - n^*\Theta \\ &= C^*\left[e_1^*(x) - \alpha^*\Theta\right] + B^*\left[\kappa_1^*(x) - \beta^*\Theta\right] \end{aligned} \tag{B1a}$$

$$\begin{aligned} M_1^*(x) &= A^*\kappa_1^*(x) + B^* e_1^*(x) - \mu^*\Theta \\ &= A^*\left[\kappa_1^*(x) - \beta^*\Theta\right] + B^*\left[e_1^*(x) - \alpha^*\Theta\right] \\ &= D^*\left[\kappa_1^*(x) - \beta^*\Theta\right] + \rho^* N_1^*(x) \end{aligned} \tag{B1b}$$

Normalized membrane force $N_2(x)$ and normalized bending moment $M_2(x)$, with respect to the reference surface, in the base structure outside the patched region are

$$N_2(x) = C[e_2(x) - \alpha\Theta] \tag{B2a}$$

$$M_2(x) = D\kappa_2(x) - \tfrac{1}{2}hN_0(x) \tag{B2b}$$

Normalized membrane and bending stiffnesses of the base-plate and the patch are

$$C = 12/h^2 \tag{B3a}$$

$$D = 1 \tag{B3b}$$

$$C_p = CE_0h_0 \tag{B3c}$$

$$D_p = E_0h_0^3 \tag{B3d}$$

$$h_0 = h_p/h \tag{B3e}$$

Modulus ratio:

$$E_0 = \bar{E}_p/\bar{E} \text{ (plane stress)} \tag{B4}$$

$$E_0 = \frac{\bar{E}_p\,|\,(1 - \nu_p^2)}{\bar{E}/(1 - \nu^2)} \text{ (plane strain)} \tag{B4'}$$

where $\bar{E}$ and $\bar{E}_p$ correspond to the dimensional elastic moduli of the base panel and patch respectively, and ν and ν_p correspond to the associated Poisson's ratios.

Ratio of coefficients of thermal expansion:

$$\alpha_0 \equiv \alpha_p/\alpha \tag{B5}$$

where for plane stress:

$$\alpha = \alpha^0 \tag{B6a}$$

$$\alpha_p = \alpha_p^0 \tag{B6b}$$

or for plane strain:

$$\alpha = (1 + \nu)\alpha^0 \tag{B6a'}$$

$$\alpha_p = (1 + \nu_p)\alpha_p^0 \tag{B6b'}$$

The nondimensional coefficients of thermal expansion of the base structure and the patch α^0 and α_p^0, respectively, are the products of the corresponding dimensional coefficients and reference temperature.

The normalized stiffnesses and thermal coefficients of the intact segment of the composite structure are

$$A^* = D + D_p + \left(\tfrac{1}{2}h\right)^2 C + \left(\tfrac{1}{2}h_p\right)^2 C_p \tag{B7a}$$

$$B^* = \tfrac{1}{2}h_p C_p - \tfrac{1}{2}hC \tag{B7b}$$

$$C^* = C + C_p \tag{B7c}$$

$$D^* = A^* - \rho^* B^* \tag{B7d}$$

$$\alpha^* = \alpha_1 - \rho^*\beta^* \tag{B7e}$$

$$\beta^* = m^*/D^* \tag{B7f}$$

where

$$\rho^* = B^*/C^* \tag{B7g}$$

$$\mu^* = \tfrac{1}{2}h_p C_p \alpha_p - \tfrac{1}{2}hC\alpha \tag{B7h}$$

$$n^* = C_p\alpha_p + C\alpha \tag{B7i}$$

$$m^* = \mu^* - \rho^* n^* \tag{B7j}$$

$$\alpha_1 = n^*/C^* \tag{B7k}$$

Appendix C: Normalized Edge Load

The normalized edge load is given by

$$T_0 = \bar{T}\bar{L}^2/\bar{D} \tag{C1}$$

where $\bar{T}$ is the dimensional in-plane load.

References

[1] Karlsson, A. M., and Bottega, W. J., "On Thermal Buckling of Patched Beam-Plates," *International Journal of Solids and Structures* (to be published).

[2] Karlsson, A. M., and Bottega, W. J., "On the Behavior of a Class of Patched Plates During Cooling," *International Journal of Non-Linear Mechanics*, Vol. 35, No. 3, 2000, pp. 543–566.

[3] Roderick, G. L., "Prediction of Cyclic Growth of Cracks and Debonds on Aluminum Sheets Reinforced with Boron/Epoxy," *Fibrous Composites in Structural Design*, Plenum, New York, 1980, pp. 467–481.

[4]Sih, G. C., and Hong, T. B., "Integrity of Edge-Debonded Patch on Cracked Panel," *Theoretical and Applied Fracture Mechanics*, Vol. 12, No. 2, 1989, pp. 121–143.

[5]Baker, A. A., "Repair Efficiency in Fatigue-Cracked Aluminum Components Reinforced with Boron/Epoxy Patches," *Fatigue and Fracture of Engineering Materials and Structures*, Vol. 66, No. 7, 1993, pp. 753–765.

[6]Bottega, W. J., "Separation Failure in a Class of Bonded Plates," *Composite Structures*, Vol. 30, No. 3, 1995, pp. 253–269.

[7]Bottega, W. J., and Loia, M. A., "Edge Debonding in Patched Cylindrical Panels," *International Journal of Solids and Structures*, Vol. 33, No. 25, 1996, pp. 3755–3777.

[8]Bottega, W. J., and Loia, M. A., "Axisymmetric Edge Debonding in Patched Plates," *International Journal of Solids and Structures*, Vol. 34, No. 18, 1997, pp. 2255–2289.

[9]Bottega, W. J., and Karlsson, A. M., "On the Detachment of Step-Tapered Doublers: Part 1—Foundations," *International Journal of Solids and Structures*, Vol. 36, No. 11, 1999, pp. 1597–1623.

[10]Karlsson, A. M., and Bottega, W. J., "On the Detachment of Step-Tapered Doublers: Part 2—Evolution of Pressure Loaded Structures," *International Journal of Solids and Structures*, Vol. 36, No. 11, 1999, pp. 1625–1651.

[11]Karlsson, A. M., and Bottega, W. J., "The Presence of Edge Contact and Its Influence on the Debonding of Patched Panels," *International Journal of Fracture*, Vol. 96, No. 4, 1999, pp. 381–404.

[12]Naboulsi, S., and Mall, S., "Thermal Effects on Adhesively Bonded Composite Repair of Cracked Aluminum Panels," *Theoretical and Applied Fracture Mechanics*, Vol. 26, No. 1, 1997, pp. 1–12.

[13]Lena, M. R., Klug, J. C., and Sun, C. T., "Composite Patches as Reinforcements and Crack Arrestors in Aircraft Structures," *Journal of Aircraft*, Vol. 35, No. 2, 1998, pp. 318–323.

[14]Timoshenko, S., "Analysis of Bi-metal Thermostats," *Journal of the Optical Society of America and Review of Scientific Instruments*, Vol. 11, No. 3, 1925, pp. 233–255.

[15]Wahl, A. M., "Analysis of Valverde Thermostat," *Journal of Applied Mechanics*, Vol. 11, No. 3, 1944, pp. A183–A189.

[16]Wittrick, W. H., "Stability of a Bimetallic Disk, Part I," *Quarterly Journal of Mechanics and Applied Mathematics*, Vol. 6, No. 1, 1953, pp. 15–26.

[17]Wittrick, W. H., Myers, D. M., and Blunden, W. R., "Stability of a Bimetallic Disk, Part II," *Quarterly Journal of Mechanics and Applied Mathematics*, Vol. 6, No. 1, 1953, pp. 26–31.

[18]Huang, N. N., and Tauchert, T. R., "Postbuckling Response of Antisymmetric Angle-Ply Laminates to Uniform Temperature Loading," *Acta Mechanica*, Vol. 72, No. 8, 1988, pp. 173–183.

[19]Hamamoto, A., and Hyer, M. W., "Non-Linear Temperature-Curvature Relationships for Unsymmetric Graphite-Epoxy Laminates," *International Journal of Solids and Structures*, Vol. 23, No. 7, 1987, pp. 919–935.

[20]Gauss, R. C., and Antman, S. S., "Large Thermal Buckling of Nonuniform Beams and Plates," *International Journal of Solids and Structures*, Vol. 20, No. 11/12, 1984, pp. 979–1000.

[21]Tauchert, T. R., "Thermally Induced Flexure, Buckling, and Vibration of Plates," *Applied Mechanics Reviews*, Vol. 44, No. 8, 1991, pp. 347–360.

[22]Noor, A. K., and Burton, W. S., "Computational Models for High-Temperature Multilayered Composite Plates and Shells," *Applied Mechanics Reviews*, Vol. 45, No. 10, 1992, pp. 419–446.

[23]Noor, A. K., and Peters, J. M., "Thermomechanical Buckling of Multilayered Composite Plates," *Journal of Engineering Mechanics*, Vol. 118, No. 2, 1992, pp. 351–366.

[24]Noor, A. K., Starnes, J. H., Jr., and Peters, J. M., "Thermomechanical Buckling and Postbuckling of Multilayered Composite Panels," *Composite Structures*, Vol. 23, No. 3, 1993, pp. 233–251.

[25]Librescu, L., and Souza, M. A., "Post-Buckling of Geometrically Imperfect Shear-Deformable Flat Panels Under Combined Thermal and Compressive Edge Loadings," *Journal of Applied Mechanics*, Vol. 60, No. 2, 1993, pp. 526–533.

[26]Singh, G., Ventkatswara Rao, G., and Iyengar, N. G. R., "Thermal Post Buckling Behavior of Rectangular Antisymmetric Cross-Ply Composite Plates," *Acta Mechanica*, Vol. 98, No. 1–4, 1993, pp. 39–50.

[27]Dano, M.-L., and Hyer, M. W., "Thermally-Induced Deformation Behavior of Unsymmetric Laminates," *International Journal of Solids and Structures*, Vol. 35, No. 17, 1998, pp. 2101–2120.

[28]Yin, W.-L., "Thermomechanical Buckling of Delaminated Composite Laminates," *International Journal of Solids and Structures*, Vol. 35, No. 20, 1998, pp. 2639–2653.

A. M. Waas
Associate Editor